# An Accurate Model for Pull-in Voltage of Circular Diaphragm Capacitive Micromachined Ultrasonic Transducers (CMUT)

Mosaddequr Rahman, Sazzadur Chowdhury
Department of Electrical and Computer Engineering
University of Windsor
Windsor, Ontario, Canada

# Research Objective

- Develop an accurate Analytical Model to calculate Pull-in Voltage of a CMUT device built with Circular diaphragm.

  CMUT devices are a type of MEMS capacitive ultrasonic sensors characterized by small device dimensions.

  The model takes into account

  - *Non-linear stretching of the diaphragm due to Large Deflection,*
  - *Built-in Residual Stress of the membrane,*
  - *Bending Stress, and*
  - *the Fringing Field effect*, and
  - *the non-linearity of the Electrostatic Field*

# Presentation Outline

- Motivation
- Basic Device Structure and Operation
- Limitations in Existing Models
- Solution Approach
- Model Development
- Model Validation
- Conclusions

# Motivation

- CMUT devices has
  - Wide Range of Applications
    - Biomedical Imaging
    - Automotive Collision Avoidance Radar System
    - Nondestructive Testing
    - Microphones
  - Superior performance over traditional piezoelectric transducers
    - low temperature sensitivity
    - high signal sensitivity
    - wide bandwidth
    - very high level of integration (low cost)

**Estimating Pull-in Voltage $V_{\text{Pull-in}}$ and the Plate Travel Distance $x_P$ before pull-in effect is required for the successful design of electrostatic actuators, switches, varactors, and sensors.**

# Basic Device Structure

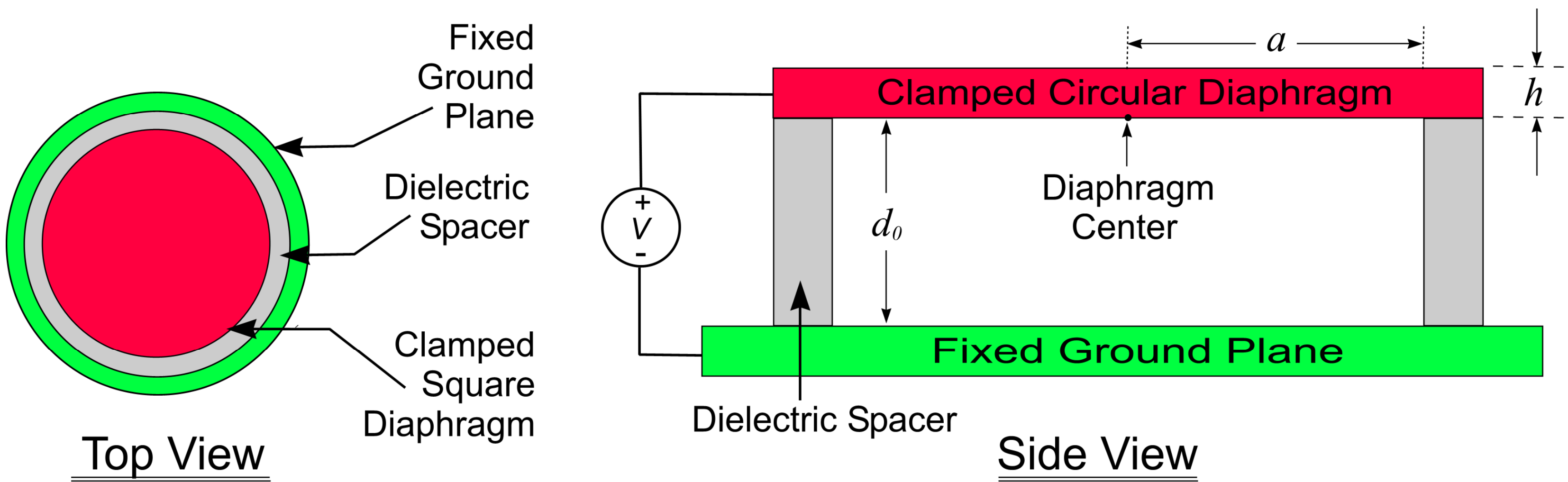


**Basic structure of a CMUT device with a circular diaphragm.**

# Operation Principle

**Diaphragm deformation after subject to an external pressure.**

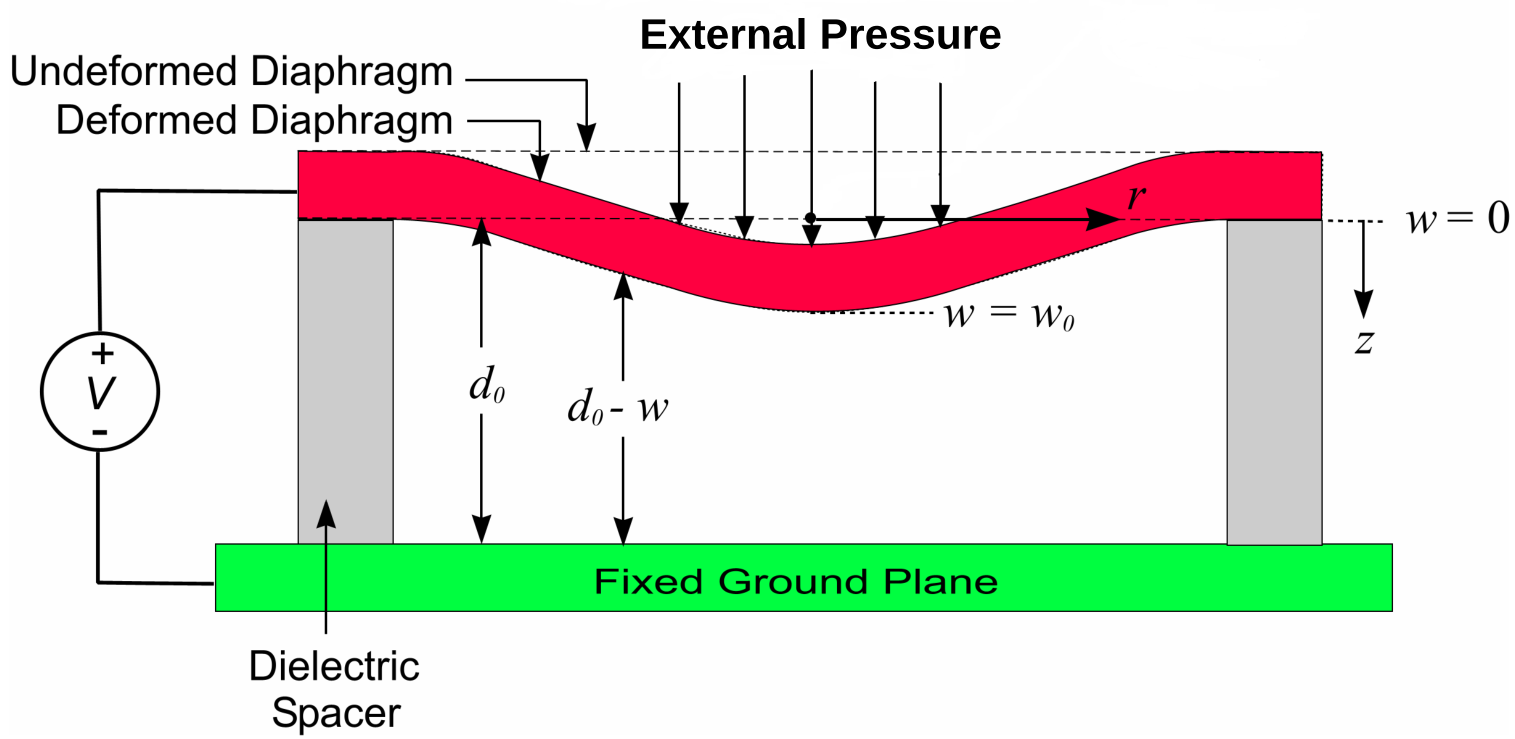


➡ *At equilibrium, Electrostatic Attraction Force is balanced by the Elastic Restoring Force of the Diaphragm*

# Diaphragm Collapse and Pull-in Voltage ($V_{Pull\text{-}in}$)

For $V < V_{\text{Pull-in}}$, *Electrostatic Force = Elastic Restoring Force*

For $V > V_{\text{Pull-in}}$, *Electrostatic Force > Elastic Restoring Force*

Diaphragm collapses under excessive electrostatic pressure

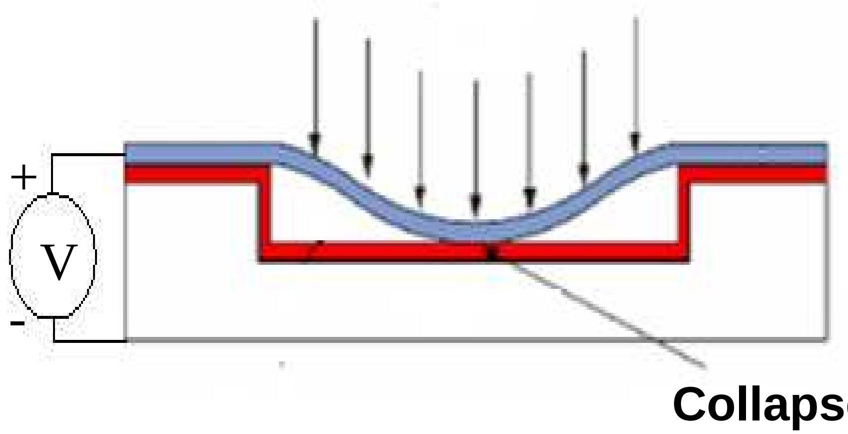

# Limitations in Existing Models: Parallel Plate Approximation

- Existing models are based on **parallel plate approximation**
- Assumes piston-like motion of the diaphragm and predicts pull-in when center deflection reaches ⅓ of the airgap

$$w_{0-\mathrm{PI}} = 1/3d_0 \quad (1)$$

Pull-in travel of the diaphragm

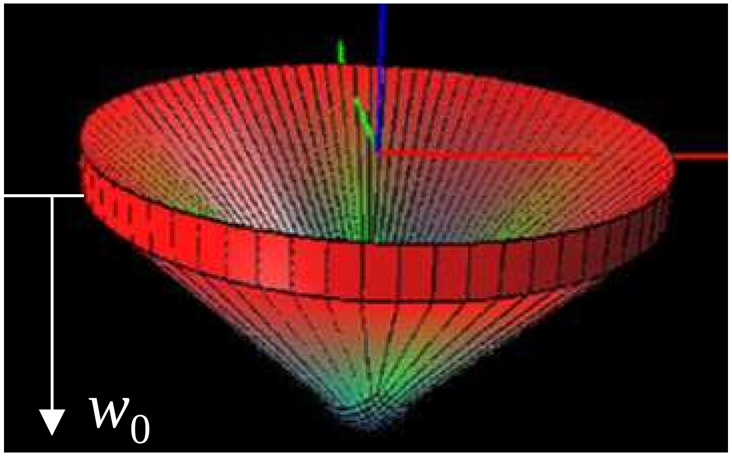


*Deflection of Circular Diaphragm in Intellisuite*

# Limitations in Existing Models: Spring Hardening Effect

- Does not account for **spring hardening effect** due to non-linear stretching of the diaphragm under **large deflection,** more pronounced in **thin diaphragms** as in CMUTs

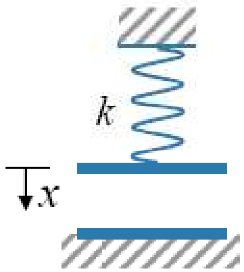


Force $F = kx$, $k$ is the spring constant

Not valid for large deflection

- Spring hardening causes the Pull-in Voltage to go up and center deflection can be as high as 50% of the airgap

$$w_{0-\mathrm{PI}} \approx 0.5 d_0 \quad (2)$$

- Does not take into account the effect of **Poisson ratio**

# Limitations in Existing Models: Fringing Field Effect

- Existing model does take into account the effect due to **Fringing Fields**
- Fringing Field effect causes **spring softening effect** of the diaphragm, lowering the pull-in voltage
- The effect is more pronounced in sensors with small diaphragm, such as in CMUT devices
- **Above simplifications results in an error as high as 20% when compared to experimental and FEA results**

# Solution Approach

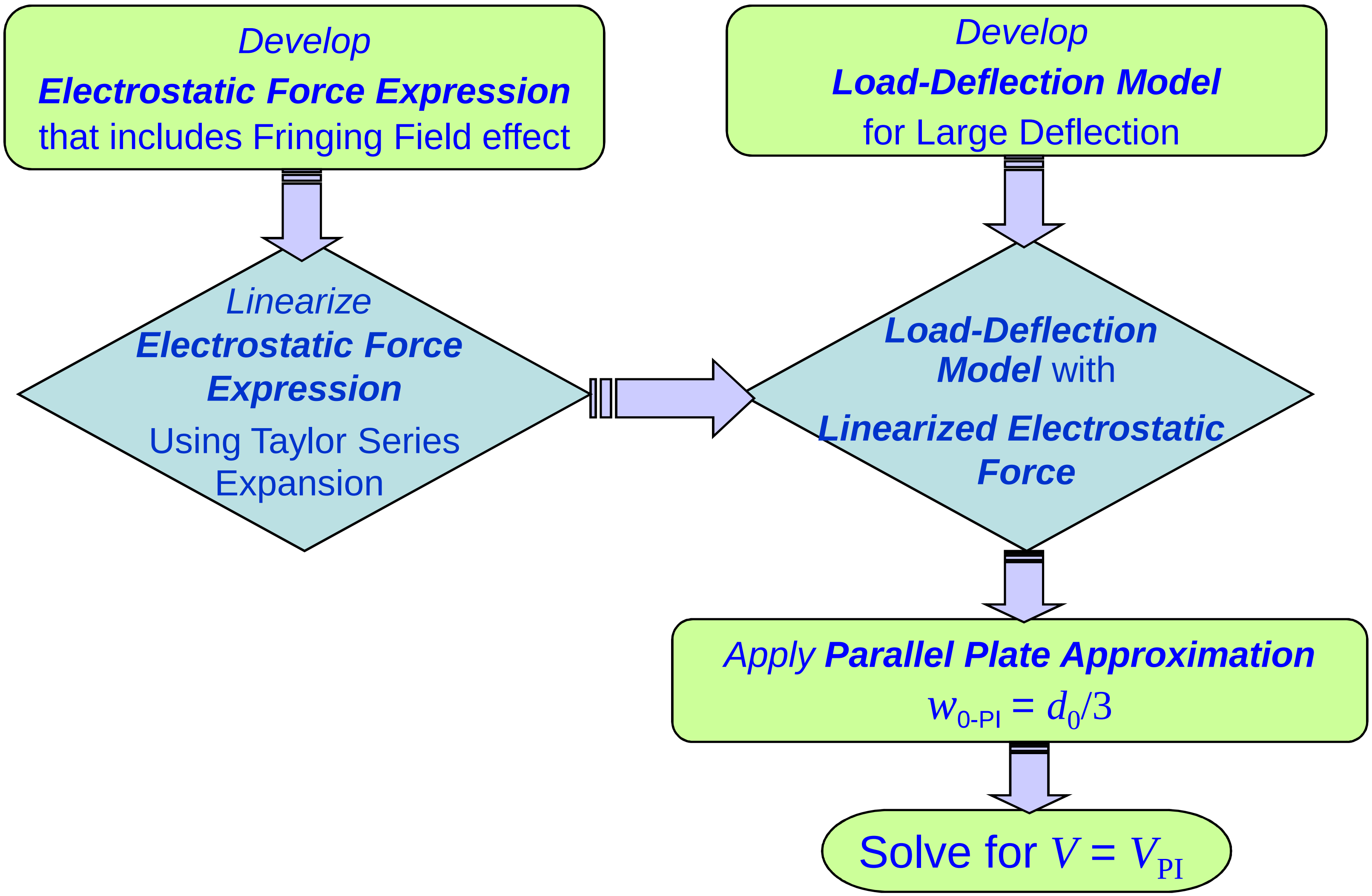

# Model Development

**Load-Deflection Model**

# Assumptions

- As the deflection of membrane is very small compared to its side-length, the *forces on the membrane are assumed to always act perpendicular* to the diaphragm surface.

- *The deflection of the membrane is assumed to be a quasistatic process*, i.e., the dynamic effects due to its motion (such as inertia force, damping force, etc) are not considered in this analysis.

# Load-Deflection Model of a Circular Membrane

Load-deflection model for circular membrane, subject to **large deflection**, due to an applied **uniform external pressure** *P*:

$$\boxed{P=\left[\frac{4\sigma_0 h}{a^2}+\frac{64D}{a^4}\right]w_o+\left[\frac{128\alpha D}{h^2a^4}\right]w_o^3} \quad * \qquad (3)$$

Combined Stiffness due to Bending and residual stress

Stiffness of the membrane due to the nonlinear stretching

$h$ ⟶ Membrane Thickness

$D=\dfrac{\tilde{E}h^3}{12(1-\nu^2)}$ ⟶ Flexural rigidity

$\tilde{E}=\dfrac{E}{1-\nu^2}$ ⟶ Effective Young's modulus

$\alpha=\dfrac{7505+4250\nu-2791\nu^2}{35280}$ ⟶ Poisson ratio dependent empirical parameter

$a$ ⟶ Membrane radius

$\sigma_0$ ⟶ Residual Stress

$E$ ⟶ Young's modulus

$\nu$ ⟶ Poisson ratio

* S. Timoshenko and S. Woinowsky-Krieger, *Theory of Plates and Shells*, McGraw-Hill Book Company New York, 1959, pp. 397-428.
M. Gad-El-Haq (Editor), MEMS Handbook, Second Edition, 2002, CRC Press, Boca Raton, pp. 3-1-3-4.

# Model Development

**Electrostatic Pressure**

# Electrostatic Force Profile

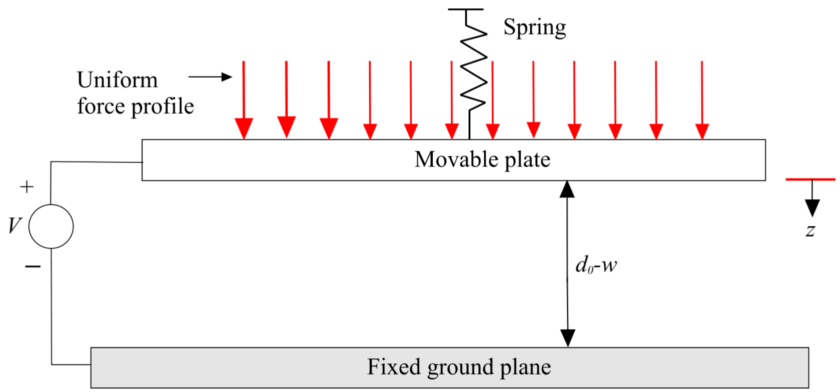


(a) Parallel plate acutator

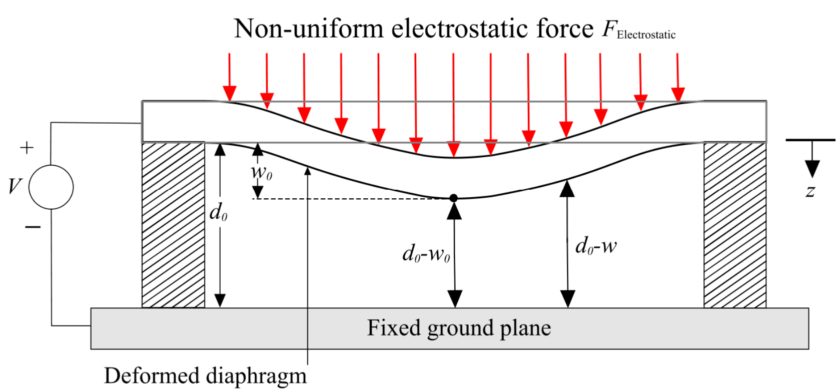


(b) Clamped diaphragm actuator

Electrostatic force profile in a parallel plate geometry:

Uniform but Non-Linear

Electrostatic force profile in a deformed clamped square diaphragm:

Non-Uniform and Non-Linear

- No known solution for Load-Deflection Model exist with non-linear non-uniform electrostatic force

# Solution Approach for Non-Linear Non-Uniform Force

Assume a **Piston-like motion** of the Diaphragm, CMUT can be approximated as **Parallel Plate Actuator**

↓

*Develop*
**Expression for Electrostatic Force**
Uniform But Non-Linear

↓

*Linearize*
**Electrostatic Force using**
Taylor Series Expansion

↓

**Uniform Linear Electrostatic Force**

# Capacitance: Undeflected Diaphragm

❖ Capacitance of undeflected diaphragm:

$$C = C_0\left(1 + C_{ff}\right) = \frac{a^2 \pi \varepsilon_r \varepsilon_0}{d_0}\left\{1 + \frac{2d_0}{\pi \varepsilon_r a}\left[\ln\left(\frac{a}{2d_0}\right) + (1.41\varepsilon_r + 1.77) + \frac{d_0}{a}(0.268\varepsilon_r + 1.65)\right]\right\} \quad (4)$$ *

$C_0 = \varepsilon_0 \varepsilon_r \pi a^2 / d_0$ ⟶ Parallel plate capacitance (5)

$C_{ff} \cong \frac{2d_0}{\pi \varepsilon_r a}\left[\ln\left(\frac{a}{2d_0}\right) + (1.41\varepsilon_r + 1.77) + \frac{d_0}{a}(0.268\varepsilon_r + 1.65)\right]$ ⟶ Fringing Field Factor (6)

$\varepsilon_0 = 8.854 \times 10^{-14}$ ⟶ Dielectric Permittivity of free space

$\varepsilon_r = 1$ (for air) ⟶ Relative Permittivity of the medium (7)

* W. C. Chew and J. A. Kong, "Effects of Fringing Fields on the Capacitance of Circular Microstrip Disk", *IEEE Transactions on Microwave Theory and Techniques*, Vol. 28, No. 2, pp. 98-104, Feb. 1980.

# Capacitance: Deflected Diaphragm

- Capacitance of deflected diaphragm for any deflection $w$:

$$C_{\text{PP-Piston}} \cong \frac{a^2 \pi \varepsilon_r \varepsilon_0}{d}\left\{1+\frac{2d}{\pi \varepsilon_r a}\left[\ln\left(\frac{a}{2d}\right)+(1.41\varepsilon_r+1.77)+\frac{d}{a}(0.268\varepsilon_r+1.65)\right]\right\} \quad (8)$$

where, $d = d_0 - w$, is the separation between the diaphragm and the backplate

| | |
|---|---|
| *Assumption made* | Piston-like motion of the diaphragm (Parallel Plate Approximation) |

- $\varepsilon_r = 1$ (for air), substituting in (8) the Capacitance expression becomes:

$$C_{\text{pp-piston}} \cong \frac{a^2 \pi \varepsilon_0}{d_0 - w}\left\{1+\frac{2(d_0-w)}{\pi\, a}\left[\ln\left(\frac{a}{2(d_0-w)}\right)+\frac{1.918(d_0-w)}{a}+3.18\right]\right\} \quad (9)$$

# Electrostatic Force

- The developed *Electrostatic Force* after applying a bias voltage $V$

$$F_{\text{electrostatic}} = -\frac{d}{dz}\left(\frac{1}{2}C_{\text{pp-piston}}V^2\right) = \left[\frac{\pi a^2}{2(d_o - w)^2} + \frac{a}{d_o - w} - 1.918\right]\varepsilon_0 V^2 \qquad (10)$$

- After Linearizing using Taylor series expansion method about the zero deflection point and rearranging the terms:

$$F_{\text{electrostatic}} = \varepsilon_0 \pi a^2 V^2 \left[\frac{1}{2d_0^2} + \frac{1}{\pi a d_0} + \frac{1.918}{\pi a^2}\right] + \varepsilon_0 \pi a^2 V^2 \left[\frac{1}{d_0^3} + \frac{1}{\pi a d_0^2}\right] w \qquad (11)$$

# Electrostatic Pressure

- Replacing $w = w_0$, the *Electrostatic Pressure* is given by,

$$P_{\text{electrostatic}} = \frac{F_{\text{electrostatic}}}{A} = \varepsilon_0 V^2 \left[ \frac{1}{2d_0^2} + \frac{1}{\pi a d_0} + \frac{1.918}{\pi a^2} \right] + \varepsilon_0 V^2 \left[ \frac{1}{d_0^3} + \frac{1}{\pi a d_0^2} \right] w_0 \qquad (12)$$

Load-deflection model due to electrostatic pressure
Yields uniform linear electrostatic pressure profile

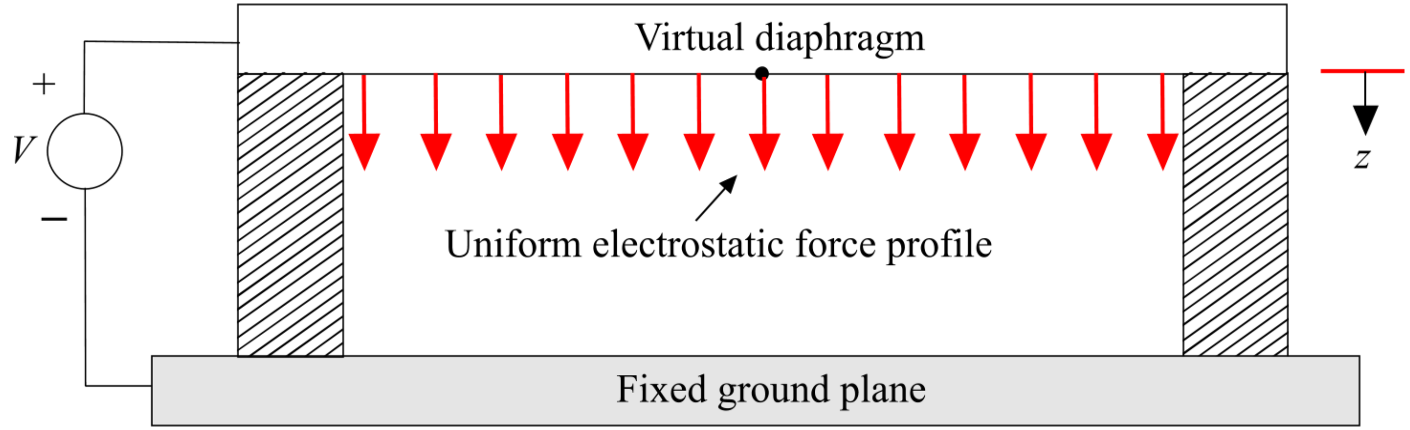


Virtual planar diaphragm after linearizng the electrostatic force about the zero deflection point of the diaphragm center

# Model Development

**Pull-in Voltage**

# Pressures on Diaphragm at Pull-in Equilibrium

- For Parallel Plate Actuator, diaphragm travel at pull-in

$$w_{0-\mathrm{PI}} = d_0/3 \tag{1}$$

- At *pull-in equilibrium,*

**1. Electrostatic Pressure** $P_{\text{PI-electrostatic}}$ (from electrostatic pressure expression) [after substituting $w_0 = d_0/3$ in (12)]:

$$P_{\mathrm{PI-electrostatic}} = \varepsilon_0 V_{\mathrm{PI}}^2 \left[\frac{1}{2d_0^2} + \frac{1}{\pi a d_0} + \frac{1.918}{\pi a^2}\right] + \varepsilon_0 V_{\mathrm{PI}}^2 \left[\frac{1}{d_0^3} + \frac{1}{\pi a d_0^2}\right]\left(\frac{d_0}{3}\right) \tag{13}$$

**2. Elastic Restoring Pressure** $P_{\text{PI-elastic}}$ (from load-deflection model) [after substituting $w_0 = d_0/3$ in (3)]

$$P_{\mathrm{PI-elastic}} = \left[\frac{64D}{a^4} + \frac{4\sigma h}{a^2}\right]\left(\frac{d_0}{3}\right) + \frac{128\alpha D}{h^2 a^4}\left(\frac{d_0}{3}\right)^3 \tag{14}$$

# Pull-in Voltage

- At *pull-in equilibrium*, the **electrostatic pressure** is just counterbalanced by the **elastic restoring pressure**

$$\boxed{P_{\mathrm{PI-electrostatic}} = P_{\mathrm{PI-elastic}}} \qquad (15)$$

- (13) and (14) can be solved simultaneously to yield the closed-form model for the pull-in voltage $V_{\mathrm{PI}}$ for the circular diaphragm as:

$$\boxed{V_{\mathrm{PI}} = \sqrt{\frac{\left[\frac{64D}{a^4} + \frac{4\sigma h}{a^2}\right]\left(\frac{d_0}{3}\right) + \frac{128\alpha D}{h^2 a^4}\left(\frac{d_0}{3}\right)^3}{\varepsilon_0\left[\frac{5}{6d_0^2} + \frac{4}{3\pi a d_0} + \frac{1.918}{\pi a^2}\right]}}} \qquad (16)$$

# Model Validation

# Finite Element Analysis Using IntelliSuite

**Table I. Device Specifications Used in FEA Simulation**

| Parameter | Unit | Value |
|---|---|---|
| Diaphragm Radius (***a***) | μm | 250 |
| Diaphragm Thickness (***h***) | μm | 1-3 |
| Airgap Thickness ($d_0$) | μm | 2-3 |
| Young's Modulus (***E***) | GPa | 169 |
| Poisson Ratio (ν) | - | 0.3 |

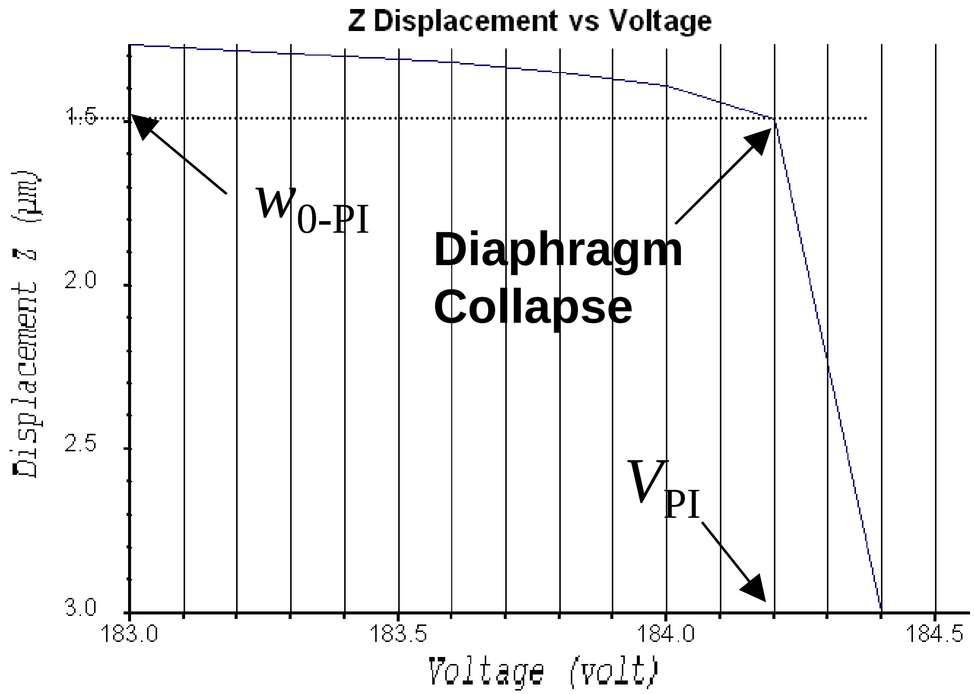


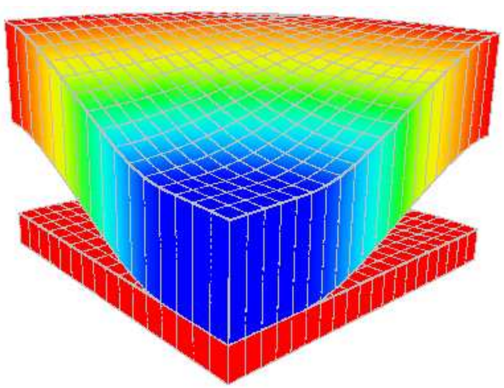

(Right) Screen capture of the diaphragm collapse after carrying out a 3-D electromechanical FEA using InteilliSuite. ($h$ = 3 μm, $d_0$= 3 μm, $\sigma_0$ = 100 MPa).

# Model Validation

## Table II. Pull-in Voltage Comparison

Diaphragm thickness, $h$ =1 μm, Airgap thickness, $d_0$ =2 μm

| Residual stress (MPa) | (V) | | | Δ% | |
|---|---|---|---|---|---|
| | New Model | Ref. [14] | FEA | FEA - New model | FEA - Ref. [14] |
| 0 | 11.03 | 9.89 | 12.4 | 10.98 | 20.24 |
| 100 | 49.24 | 50.48 | 49.9 | 1.3 | 1.16 |
| 250 | 76.69 | 77.88 | 76.86 | 0.22 | 1.32 |
| 350 | 90.46 | 91.56 | 90.4 | 0.074 | 1.28 |
| **Diaphragm thickness, $h$ =1 μm, Airgap thickness, $d_0$ =3 μm** | | | | | |
| 0 | 22.38 | 18.17 | 28.04 | 20.17 | 35.2 |
| 100 | 90.88 | 92.83 | 91.4 | 0.56 | 1.46 |
| 250 | 141.06 | 143.07 | 139.9 | 0.82 | 2.26 |
| 350 | 166.3 | 168.2 | 164.4 | 1.15 | 2.31 |

Ref [14] P. M. Osterberg, "Electrostatically Actuated Microelectromechanical Test Structures for Material property Measurements," *Ph.D. Dissertation*, MIT, Cambridge, MA, 1995, pp. 52-87.

# Model Validation

## Table III. Pull-in Voltage Comparison

Diaphragm thickness, $h$ =2 μm, Airgap thickness, $d_0$ =3 μm

| Residual stress (MPa) | (V) | | | Δ% | |
|---|---|---|---|---|---|
| | New Model | Ref. [14] | FEA | FEA - New model | FEA - Ref. [14] |
| 0 | 55.03 | 51.39 | 57.6 | 4.45 | 10.77 |
| 100 | 136.18 | 141.18 | 138.4 | 1.6 | 2.0 |
| 250 | 204.5 | 211.24 | 205.6 | 0.53 | 2.74 |
| 350 | 239.45 | 246.53 | 239.8 | 0.15 | 2.8 |
| Diaphragm thickness, $h$ =3 μm, Airgap thickness, $d_0$ =3 μm | | | | | |
| 0 | 98.03 | 94.42 | 97.7 | 0.33 | 3.36 |
| 100 | 181.34 | 188.14 | 184.2 | 1.55 | 2.14 |
| 250 | 260.38 | 271.20 | 263.4 | 1.14 | 2.96 |
| 350 | 301.78 | 313.77 | 304.4 | 0.85 | 3.07 |

Ref [14] P. M. Osterberg, "Electrostatically Actuated Microelectromechanical Test Structures for Material property Measurements," *Ph.D. Dissertation*, MIT, Cambridge, MA, 1995, pp. 52-87.

# Model Validation

## Pull-in Voltage *vs* Diaphragm Radius ($\sigma_0$>0)

(Diaphragm thickness, $h$ =3 μm, Airgap thickness, $d_0$ =3 μm , Residual stress $\sigma_0$=250 MPa)

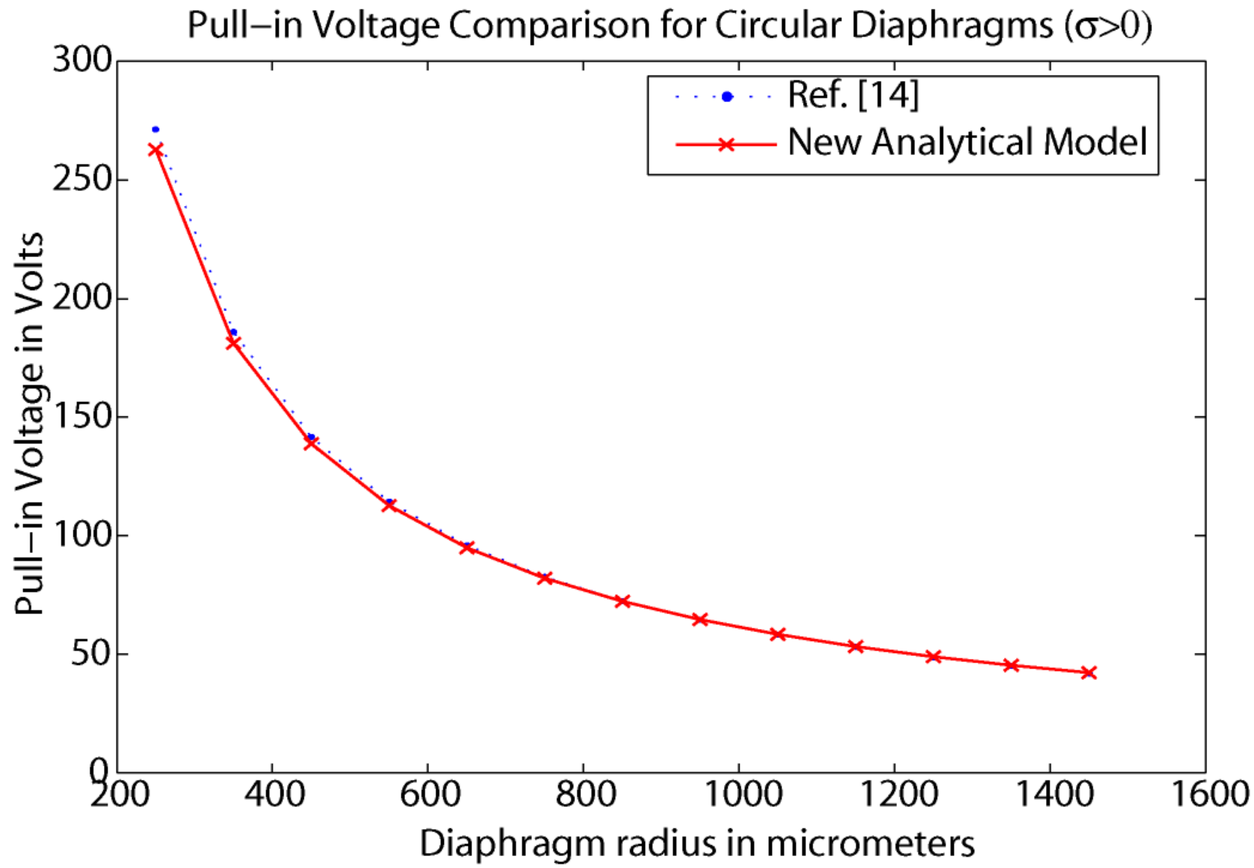


- **Both the models merge at large diaphragm radius**

# Model Validation

## Pull-in Voltage *vs* Diaphragm Radius ($\sigma_0$=0)

(Diaphragm thickness, $h$ =3 µm, Airgap thickness, $d_0$ =3 µm , Residual stress $\sigma_0$=0)

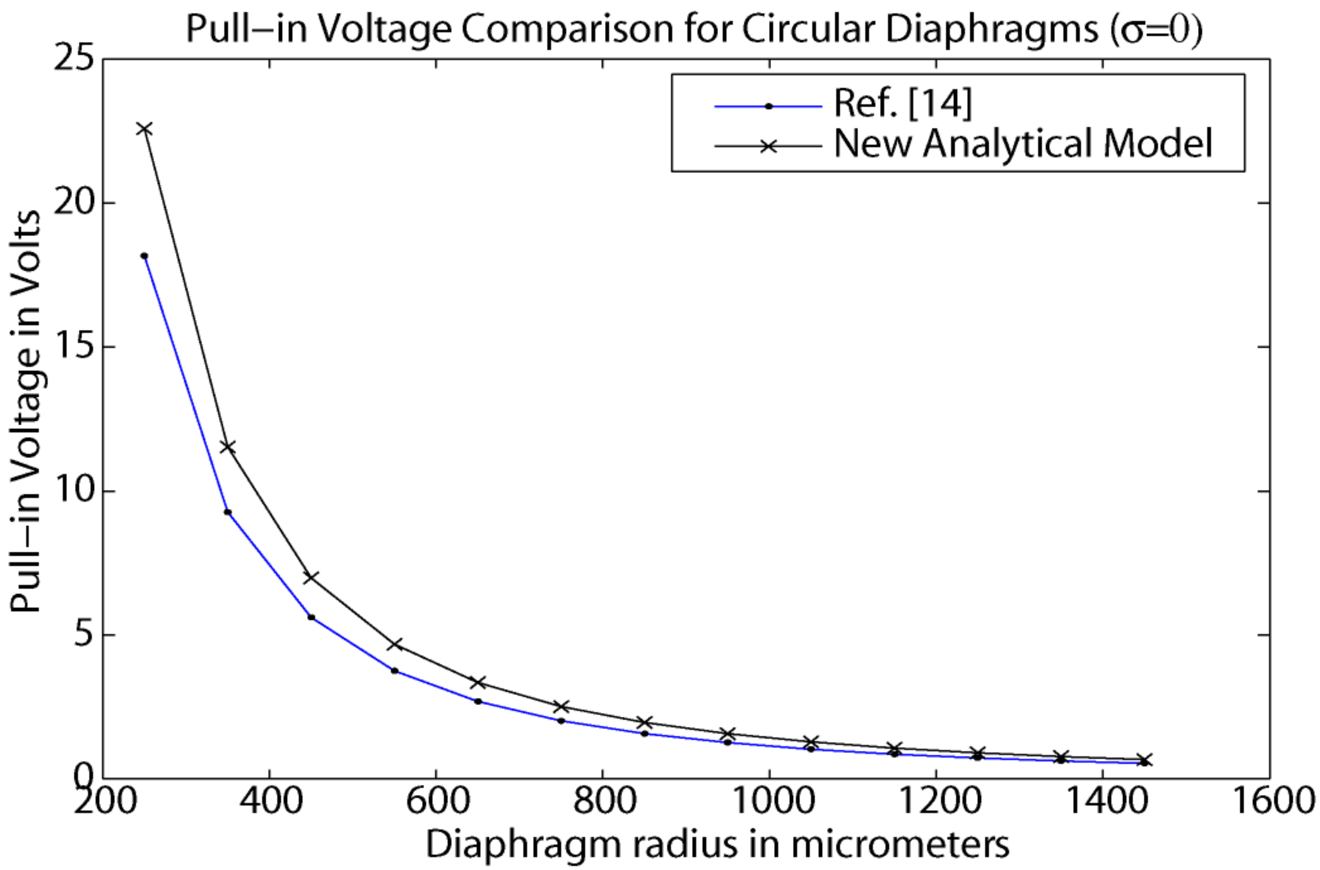


- **Both the models merge at large diaphragm radius**

# Model Limitations

The new analytical method can provide very good approximation of pull-in voltage for the following limited cases:

- Both the electrodes are required to be parallel prior to any electrostatic actuation.
- The gap between the clamped diaphragm and the backplate should be small enough so that the Taylor series expansion about the zero deflection point doesn't introduce any significant error.
- The lateral dimensions of the diaphragm are required to be very large compared to the diaphragm's thickness and the airgap.

# Conclusions

- A **highly accurate closed-form model** for the **pull-in voltage** of a clamped circular diaphragm CMUT device is presented.
- The model is **simple, easy to use** and **fast**, and takes into account both the **non-linear stretching due to large deflection** and the **non-linearity of electrostatic field**.
- Excellent agreement with 3-D electromechanical FEA using IntelliSuite with a **maximum deviation of 1.6%** for diaphragms with residual stress
- Can also be easily extended to a *Clamped-edge Square Membrane*.
- Besides CMUTs, the Model will also be useful in **ensuring safe and efficient operation** of
    - MEMS capacitive type pressure sensors
    - MEMS based microphones
    - Touch mode pressure sensors
    - Other application areas where electrostatically actuated circular diaphragms are used.

*Thanks for your Patience*